PAPER

Influences of group velocity dispersion on ultrafast pulse shaping in time lens

IOP Publishing Physica Scripta
Phys. Scr. 94 (2019) 125503 (6pp) https://doi.org/10.1088/1402-4896/ab33d0

Influences of group velocity dispersion on ultrafast pulse shaping in time lens

Peng Xie[1,2,3,4,6], **Yu Wen**[5], **Zishen Wan**[2,3] **and Yishan Wang**[1,4]

[1] State Key Laboratory of Transient Optics and Photonics, Xi'an Institute of Optics and Precision Mechanics, Chinese Academy of Sciences, Xi'an 710119, People's Republic of China
[2] Department of Mechanical Engineering, Massachusetts Institute of Technology, Cambridge 02139, United States of America
[3] School of Engineering and Applied Sciences, Harvard University, Cambridge 02138, United States of America
[4] University of Chinese Academy of Sciences, Beijing 100049, People's Republic of China
[5] National University of Defence Technology, Changsha, 410073, People's Republic of China

E-mail: pengxie@mit.edu and zishenwan@g.harvard.edu

Received 10 April 2019, revised 18 July 2019
Accepted for publication 19 July 2019
Published 5 September 2019

Abstract

Time-lens technology is of significant interest in signal processing and optical communication. The impacts of group velocity dispersion (GVD) on ultrafast pulse shaping in a time-lens system based on four-wave mixing are explored in this paper. The output signals of temporal magnification and time-to-frequency conversion under different GVDs are theoretically investigated in detail. The simulation results imply that the femtosecond pulse is sensitive to GVD in propagation. GVD has an important effect on nonlinear parametric processes, which results in output signals presenting different pulse shapes and different frequency profiles. Furthermore, a model of silicon nitride waveguide with flat dispersion is proposed by finite element method and signal processing with negligible pulse distortion is realized in near-infrared region.

Keywords: group velocity dispersion, time lens, signal processing, integrated optics

(Some figures may appear in colour only in the online journal)

1. Introduction

The duality between the paraxial diffraction of light beams in space and the dispersion of optical pulses in media contributes to the concept that an element introducing a quadratic phase shift in time is an analogy of a thin lens in space [1–4]. Based on this theory, time-lens system enters into the vision of researchers, which is an analogy of the conventional lens in the time-domain. In the past decade, time-lens system has attracted increasing attention for its promising applications in ultrafast signal processing [5, 6], data transmission [7], measurement of ultrafast signal [8, 9]. Especially, chip-integrated time lens system becomes a hotspot for significant potentials in optical processing and future all-optical communication system. Meanwhile, various methods have been developed for realizing time-lens, such as electro-optic phase modulation [10], sum-frequency or differential frequency generation [11], cross-phase modulation [12] and four-wave mixing (FWM) [13, 14]. Nowadays, the approach based on FWM is the main way to explore time-lens. Because FWM can be applied to most materials [15] and provide a precise quadratic phase [16]. What is more, FWM exhibits natural advantages in all-optical communications for its input and output signals are similar in wavelength [17]. As is well known, when ultrafast pulses propagate in fiber, the dispersion of fiber may broaden or compress the pulses [18]. As for integrated chips, the influence of the dispersion to ultrafast signal is still an interesting question and it is necessary to take it into account when doing research about signal processing. For nonlinear parametric process as FWM, GVD affects the phase-match to interfere with the signal propagation process [19]. It plays an important role in effective FWM, which leads

[6] Author to whom any correspondence should be addressed.

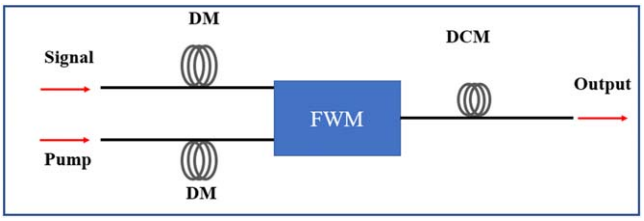

Figure 1. The scheme of time-lens system based on FWM. DM: dispersion medium. DCM: dispersion compensation medium.

to totally different output signals with different frequency profiles and waveforms. Therefore, we mainly focus on GVD and explore its impacts on time-lens system in this work. Temporal magnification and time-to-frequency conversion based on time-lens are investigated under the different GVDs and the output signals are analyzed in detail about pulse shapes and frequency elements. Besides, we propose a model of silicon nitride strip waveguide with good dispersion performance to create a time-lens system, which can contribute to ultrafast signal processing with negligible pulse distortion in near-infrared region. These results exhibit great potential in integrated optics and optical communication.

2. Numerical simulation and analysis

Figure 1 shows the principle of time-lens system based on FWM. The pump and input signal propagate through a dispersive medium (DM), respectively and then are coupled into a nonlinear medium for interaction between light and media. The input signal with an electric field amplitude $E_s(t)$ is mixed with the pump with an electric field amplitude $E_p(t)$ via the FWM, in which the generated idler is $E_i(t) \propto E_p^{\ 2}(t) \times E_s^{\ *}(t)$ and a quadratic phase $\varnothing_{f(t)}$ is imparted to the input signal [20, 21]. If the idler is detected, we can obtain the results of time-to-frequency conversion. On the other hand, if the idler propagates through the dispersion compensation medium (DCM) for dispersion compensation, the output signal will keep the same features as the input signal, which is rebuilt via a magnification factor by the time lens. As for the DM or DCM, there are several options, such as single-mode fiber, fiber Bragg grating or dispersion modules [22]. SMF is popular for its simplification.

In this work, we theoretically investigate the influences of GVD on ultrafast pulse shaping in time lens by solving following coupled mode equations [23, 24]

$$\begin{aligned}&\frac{\partial A_p}{\partial z} + \mathrm{i}\frac{1}{2}\beta_{2p}\frac{\partial^2 A_p}{\partial T^2} - \frac{1}{6}\beta_{3p}\frac{\partial^3 A_P}{\partial T^3} \\ &= -\frac{1}{2}\alpha_p A_p + \mathrm{i}\gamma_p |A_p|^2 A_p \\ &\quad + \mathrm{i}2\gamma_p(|A_s|^2 + |A_i|^2)A_p + \mathrm{i}2\gamma_p A_s A_i A_p^* \exp(\mathrm{i}\Delta\beta z),\end{aligned} \tag{1}$$

$$\begin{aligned}&\frac{\partial A_s}{\partial z} + \mathrm{i}\frac{1}{2}\beta_{2s}\frac{\partial^2 A_s}{\partial T^2} - \frac{1}{6}\beta_{3s}\frac{\partial^3 A_s}{\partial T^3} + d_s\frac{\partial A_s}{\partial T} \\ &= -\frac{1}{2}\alpha_s A_s + \mathrm{i}\gamma_s |A_s|^2 A_s \\ &\quad + \mathrm{i}2\gamma_s(|A_p|^2 + |A_i|^2)A_s + \mathrm{i}\gamma_s A_p^2 A_i^* \exp(-\mathrm{i}\Delta\beta z),\end{aligned} \tag{2}$$

$$\begin{aligned}&\frac{\partial A_i}{\partial z} + \mathrm{i}\frac{1}{2}\beta_{2i}\frac{\partial^2 A_i}{\partial T^2} - \frac{1}{6}\beta_{3i}\frac{\partial^3 A_i}{\partial T^3} + d_i\frac{\partial A_i}{\partial T} \\ &= -\frac{1}{2}\alpha_i A_i + \mathrm{i}\gamma_i |A_i|^2 A_i \\ &\quad + \mathrm{i}2\gamma_i(|A_p|^2 + |A_s|^2)A_i + \mathrm{i}\gamma_i A_p^2 A_s^* \exp(-\mathrm{i}\Delta\beta z),\end{aligned} \tag{3}$$

Where A_m is the amplitude ($m = p, s, i$), α_m is the linear loss ($m = p, s, i$). and Z is the propagation distance. The walk-off parameters for the signal and idler are defined as $d_s = \beta_{1s} - \beta_{1p}$ and $d_i = \beta_{1i} - \beta_{1p}$, respectively.$\beta_n$is calculated via numerical differentiation from $\beta_n = \mathrm{d}^n\beta/\mathrm{d}\omega^n$.

Figures 2(a), (c) shows the temporal waveform and frequency spectrum of the input signal, respectively. It is a signal consisting of two 100 fs pulses separated by 300 fs with the central wavelength at 1540 nm. Figures 2 (b), (d) shows the temporal waveform and frequency spectrum of the pump, respectively. It is a signal pulse of 40 fs with the central wavelength at 1560 nm. The result of input signal after propagating through a DM is shown in figure 2(e). The result of pump after propagating through a DM is shown in figure 2(f). The DMs of signal and pump paths are set as 100 m and 200 m SMF, respectively. According to the presented results, the pulses are broadened for the dispersion of the SMF. After FWM process, the idler is sent into 20 km dispersion compensation fiber and the output is presented in figures 2(g), (h), including temporal waveform and frequency spectrum of output signal based on temporal magnification. There are 5 pulse curves with different colors in a picture, which means that different GVD values are taken into account (black: 0 ps$^{\hat{}}$2 m^{-1}; red:−0.1 ps$^{\hat{}}$2 m^{-1}; pink:−0.2 ps$^{\hat{}}$2 m^{-1}; blue: −0.3 ps$^{\hat{}}$2 m^{-1}; azure: −0.4 ps$^{\hat{}}$2 m^{-1}). As we can see from the results, ultrafast pulse shaping is sensitive to the GVD. When $\beta_2 = 0$ ps$^{\hat{}}$2 m^{-1}, it is under ideal condition, so the result performs perfectly with a magnification factor. Furthermore, it is found that the waveform is changed with the shift of GVD in time domain. For frequency domain, the waveform is also shifted, which means the energy of frequency element is shifted. However, we can find that the frequency element is almost stable.

On the other hand, for time-to-frequency conversion, the idlers taking different GVD into account, which are similar to temporal magnification, are presented in figure 3. Figures 3(a), (b) shows temporal waveform of output signal and frequency spectrum of output signal based on time-to-frequency conversion, respectively. First, we can find that the frequency spectrum of time-to-frequency conversion is almost similar to temporal magnification. Thus, we can conclude that extra dispersion will make negligible effect on frequency

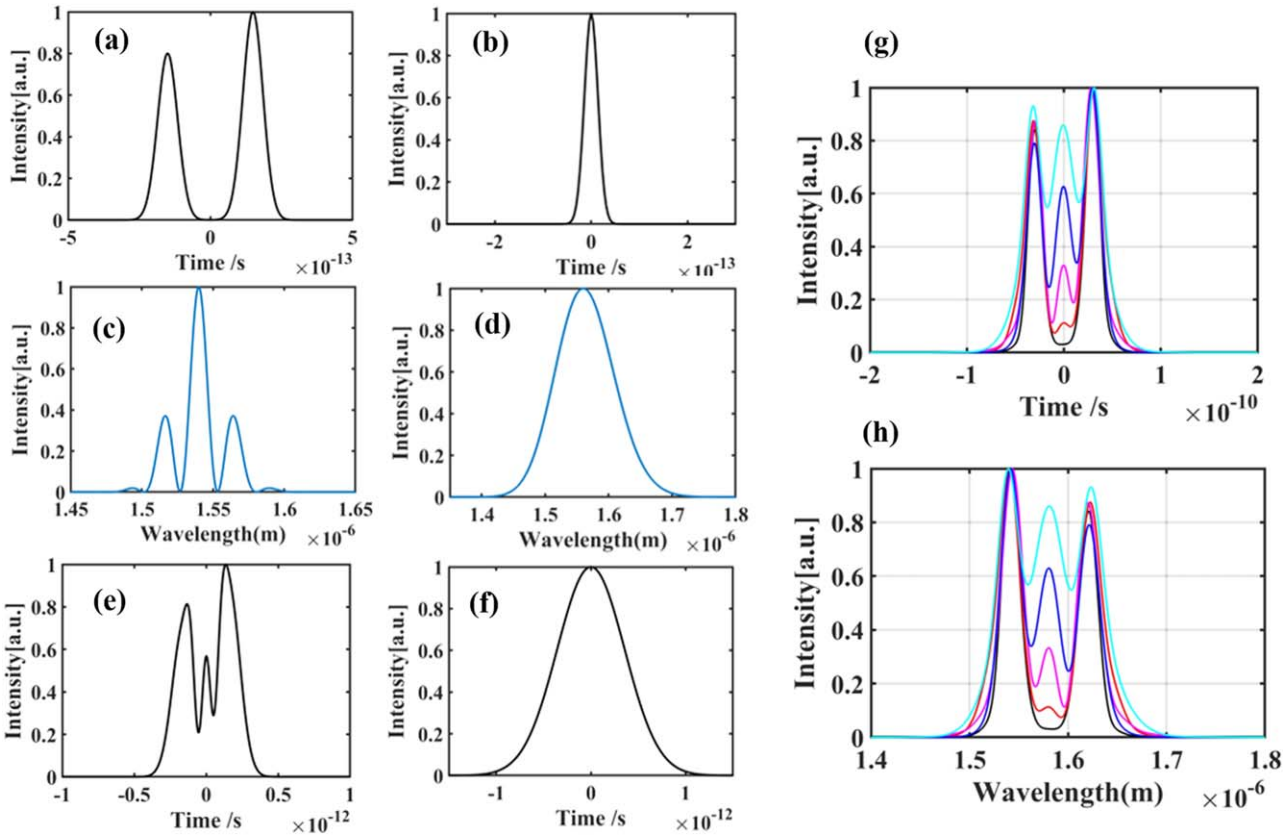

Figure 2. (a) Temporal waveform and (c) frequency spectrum of the input signal. (b) Temporal waveform and (d) frequency spectrum of the pump. (e) Temporal waveform after DM of the input signal and (f) Temporal waveform after DM of the pump. (g) Temporal waveform and (h) frequency spectrum of output signal based on temporal magnification under the GVD of 0 $ps^{\hat{}}2\,m^{-1}$, $-0.1\ ps^{\hat{}}2\,m^{-1}$, $-0.2\ ps^{\hat{}}2\,m^{-1}$, $-0.3\ ps^{\hat{}}2\,m^{-1}$, $-0.4\ ps^{\hat{}}2\,m^{-1}$, respectively.

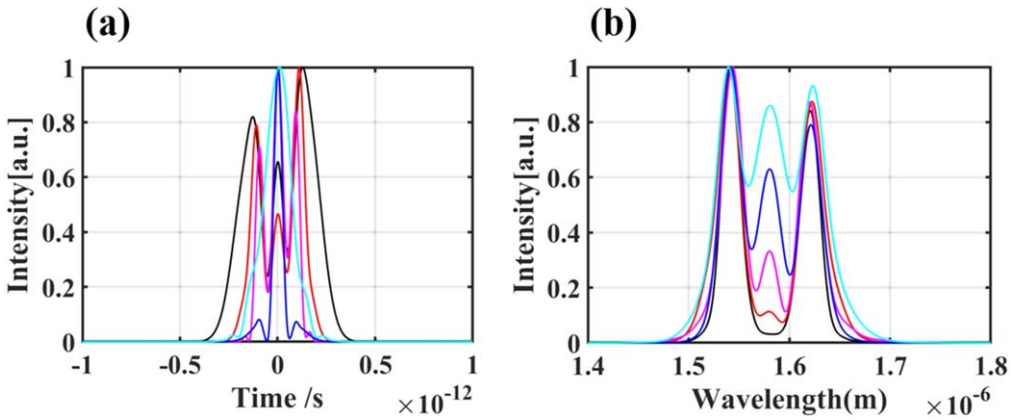

Figure 3. (a) Temporal waveform and (h) frequency spectrum of output signal based on time-to-frequency conversion.

profiles. However, the temporal waveform is totally different. Pulse shape is sharply changed with the GVD shifted. There is a regularity that the energy will be focused around central wavelength with the increase of GVD value. According to all of numerical simulations, we conclude that GVD from nonlinear medium has significant effect on pulse shaping in time lens. Therefore, it is important for time-lens system to build a nonlinear waveguide with flat GVD curves and decrease the negative impacts of GVD.

3. Device design and results

Silicon nitride (Si_3N_4) is an attractive candidate for photonic integration for its high nonlinearity and transparent in a large wavelength range [25, 26]. Here, we simulate a model of silicon nitride strip waveguide by finite element method, which is shown in figure 4(a). The core material (Si_3N_4) is around by silica, the height $h = 0.85\ \mu$m, the widths of top edge and bottom edge are set as $1.15\ \mu$m and $1.2\ \mu$m,

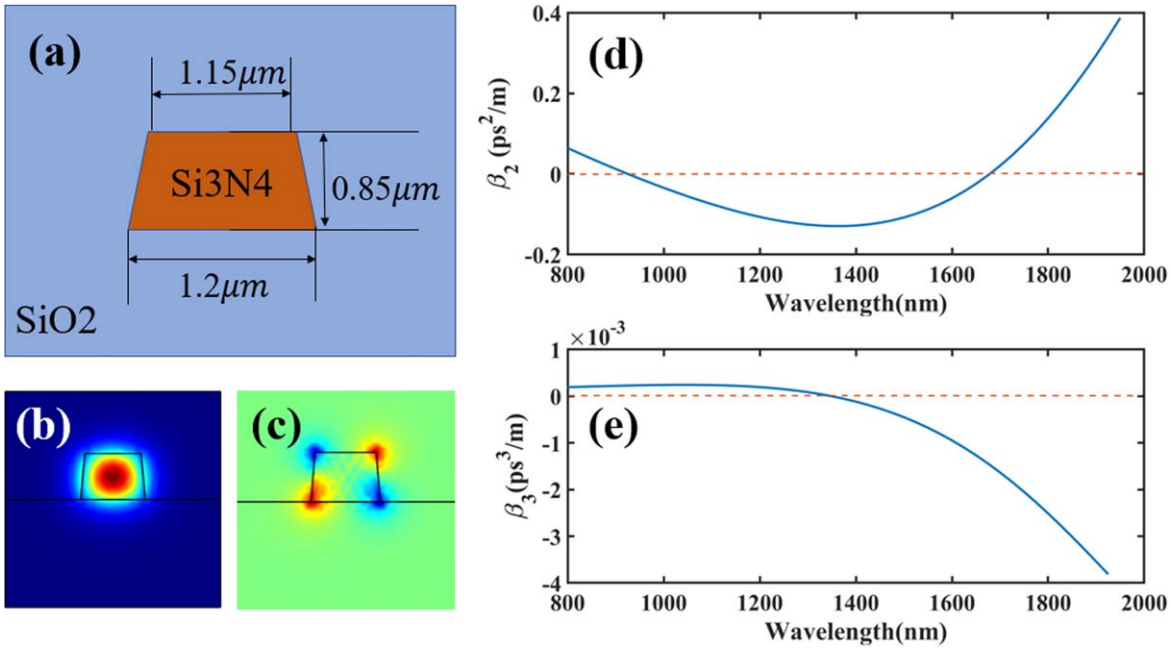

Figure 4. (a) The cross-section of the waveguide and (b) *Ex* and (c) *Ey* electric field components of the waveguide at the wavelength of 1550 nm. (d) the GVD and (e) third-order dispersion of the waveguide.

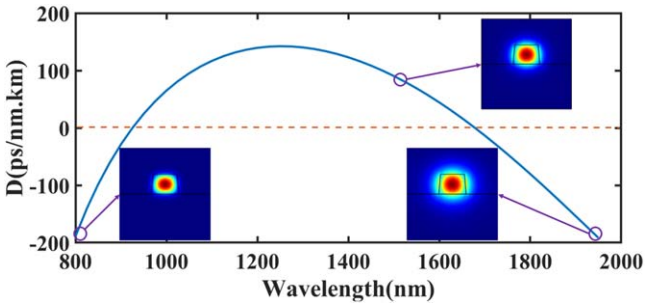

Figure 5. (a) The dispersion of the waveguide in near-infrared region and the TM modes of 800 nm, 1550 nm and 2000 nm, respectively.

respectively. The *Ex* and *Ey* electric field components of the waveguide at the wavelength of 1550 nm are shown in figures 4(b) and (c), respectively. The mode is a standard single mode and the most of energy is confined in the core material. Figures 4(d), (e) presents the GVD and three-order dispersion of the waveguide in near-infrared region.

Furthermore, we present the dispersion and TM mode in different wavelengths of the waveguide in figure 5. As we can know from the picture, the waveguide exhibits great bandwidth (about 800 nm) in near-infrared region for phase-match of the nonlinear parametric process. We present the TM modes of wavelength at 800 nm, 1550 nm and 2000 nm, respectively. The modes exhibit great performance at a single mode. On the other hand, it is obvious that the waveguide presents stronger confinement of light for shorter wavelength. With the increase of working wavelength, more energy will be distributed into the cladding material. According to the simulation by finite element method, it is not a big problem with negligible impact. At least, for this waveguide, the influence is slight in near-infrared region.

Based on the proposed Si_3N_4 strip waveguide, we explore temporal magnification and time-to-frequency conversion via time-lens system shown in figure 1. Here, we set input signal as 1540 nm and pump as 1560 nm. The GVDs to the wavelength of signal and pump are $-0.082\ \mathrm{ps}^{\hat{}2}\,\mathrm{m}^{-1}$ and $-0.071\ \mathrm{ps}^{\hat{}2}\,\mathrm{m}^{-1}$. And we mainly pay attention to the pulse shaping in this section as shown in figure 6. Temporal waveform and frequency spectrum of the input signal are based on the same parameters with previous simulation shown in figures 6(a), (b). And figures 6(c)–(f) presents the temporal waveform and frequency spectrum of output signal based on time-to-frequency conversion and temporal magnification, respectively. The results have good match to expectable theoretical results. As a whole, the curves of output is smooth with negligible distortion. For temporal magnification, the output signal keeps the similar features with input signal in pulse shape after a magnification factor of 200×. For time-to-frequency conversion, the result also meets the basic theory.

4. Conclusion

In summary, we have demonstrated the impacts of group velocity dispersion on ultrafast pulse shaping in time-lens system and presented the simulation results via solving coupled mode equation. Meanwhile, the influences of GVD on pulses about temporal magnification and time-to-frequency conversion are discussed in detail. Furthermore, a silicon nitride strip waveguide with optimal dimensions and dispersion characteristics is proposed to realize a time-lens system, which obtains excellent outputs in simulation. This work further demonstrates that the dispersion characteristics of

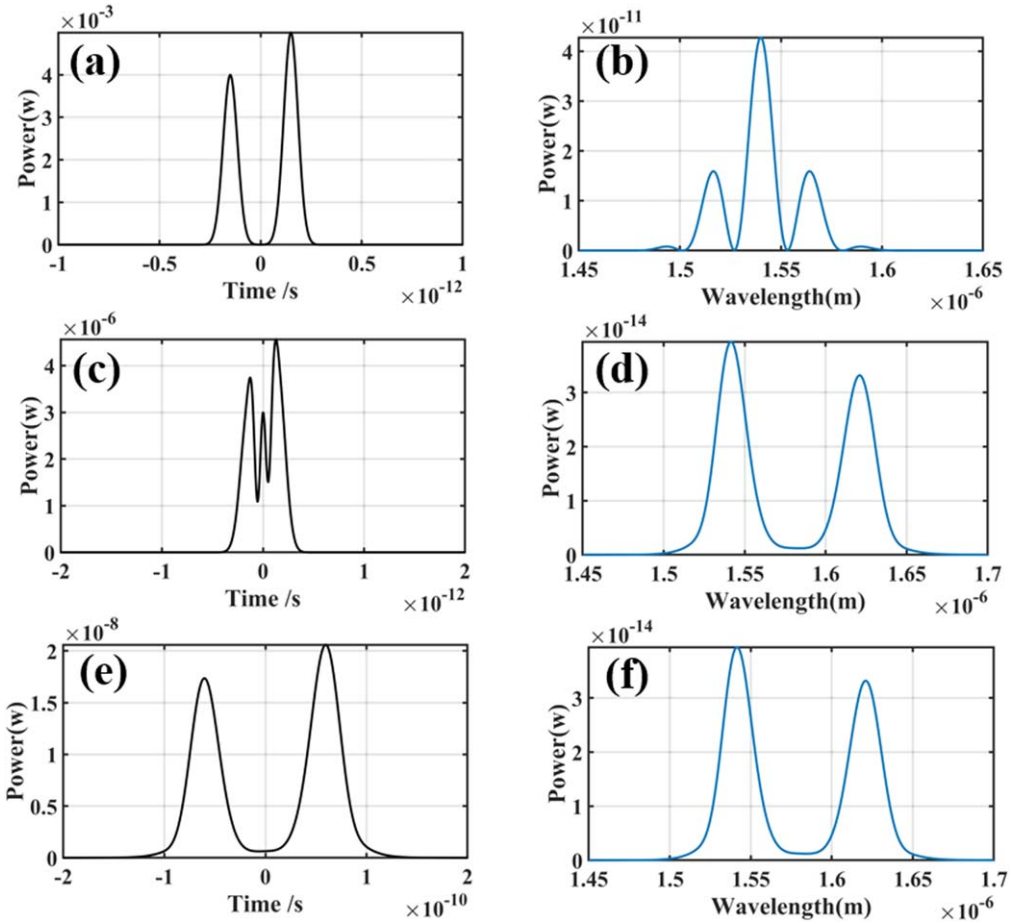

Figure 6. (a) Temporal waveform and (b) frequency spectrum of the input signal. (c) Temporal waveform and (d) frequency spectrum of the output signal based on time-to-frequency conversion. (e) Temporal waveform and (f) frequency spectrum of output signal based on temporal magnification.

nonlinear waveguide could be carefully designed to improve the performance of chip-integrated time-lens system. These results exhibit a significant potential in all-optical communication system.

Acknowledgments

This work was supported by the Strategic Priority Research Program of the Chinese Academy of Sciences (Grant No. XDB24030600) and China Scholarship Council.

ORCID iDs

Peng Xie https://orcid.org/0000-0002-3636-3001

References

[1] Foster M A, Salem R, Geraghty D F, Turner-Foster A C, Lipson M and Gaeta A L 2008 Silicon-chip-based ultrafast optical oscilloscope *Nature* **456** 81–4

[2] Kolner B H 1994 Space–time duality and the theory of temporal imaging *IEEE J. Quantum Electron.* **30** 1951–63

[3] Bennett C V, Scott R P and Kolner B H 1994 Temporal magnification and reversal of 100 gb/s optical data with an up-conversion time microscope *Appl. Phys. Lett.* **65** 2513

[4] Kauffman M T, Banyai W C, Godil A A and Bloom D M 1994 Time-to-frequency converter for measuring picosecond optical pulses *Appl. Phys. Lett.* **64** 270–2

[5] Van Howe J and Xu C 2006 Ultrafast optical signal processing based upon space–time dualities *J. Lightwave Technol.* **24** 2649–62

[6] Chembo Y K, Hmima A, Lacourt P A, Larger L and Dudley J M 2009 Generation of ultralow jitter optical pulses using optoelectronic oscillators with time-lens soliton-assisted compression *J. Lightwave Technol.* **27** 5160–7

[7] Guan P, Røge K M, Morioka T and Oxenlowe L K 2016 Time lens based optical fourier transformation for advanced processing of spectrally-efficient ofdm and n-wdm signals *Optical Fiber Communication Conference and Exhibition*

[8] Pasquazi A, Park Y Y, Chu S T, Little B E and Morandotti R 2012 Time-lens measurement of subpicosecond optical pulses in cmos compatible high-index glass waveguides *IEEE J. Sel. Top. Quantum Electron.* **18** 629–36

[9] Hugues G D C and Romero C L 2016 Optical real-time fourier transformation with kilohertz resolutions *Optica* **3** 1

[10] Karpiński M, Jachura M, Wright L J and Smith B J 2016 Bandwidth manipulation of quantum light by an electro-optic time lens *Nat. Photon.* **11** 53
[11] Tikan A, Bielawski S, Szwaj C, Randoux S and Suret P 2018 Single-shot measurement of phase and amplitude by using a heterodyne time-lens system and ultrafast digital time-holography *Nat. Photon.* **14** 228
[12] Huh J and Azana J 2017 All-optical reconfigurable signal processing based on cross phase modulation time lensing *IEEE Photonics Technol. Lett.* **29** 826–9
[13] Klein A, Shahal S, Masri G, Duadi H and Fridman M 2017 Four wave mixing-based time lens for orthogonal polarized input signals *IEEE Photonics J.* **9** 1–7
[14] Xie P, Sun Q, Wang L, Wen Y, Wang X, Wang G and Lu Z 2018 Impact of two-photon absorption and free-carrier effects on time lens based on four-wave mixing in silicon waveguides *Appl. Phys. Express* **11** 082204
[15] Sanvitto D and Kéna-Cohen S 2016 The road towards polaritonic devices *Nat. Mater.* **15** 1061–73
[16] Muellner P, Wellenzohn M and Hainberger R 2009 Nonlinearity of optimized silicon photonic slot waveguides *Opt. Express* **17** 9282–7
[17] Pasquazi A, Ahmad R, Rochett M and Lamont M 2010 All optical wavelength conversion in an integrated ring resonator *Opt. Express* **18** 3858
[18] Liu X, Cui Y, Han D, Yao X and Sun Z 2015 Distributed ultrafast fibre laser *Sci. Rep.* **5** 9101
[19] Liang W, Savchenkov A A, Ilchenko V S, Eliyahu D, Matsko A B and Maleki L 2017 Wide band parametric optical processes in crystalline microresonators *Photonics Society Summer Topical Meeting Series* (https://doi.org/10.1109/PHOSST.2017.8012629)
[20] Salem R, Foster M A, Turner A C, Geraghty D F, Lipson M and Gaeta A L 2008 Optical time lens based on four-wave mixing on a silicon chip *Opt. Lett.* **33** 1047
[21] Kolner B H and Nazarathy M 1989 Temporal imaging with a time lens *Opt. Lett.* **14** 630
[22] Xie P, Wen Y, Wan S Z, Wang X, Liu J, Yang Q W and Wang Y S 2019 Electrically tunable temporal imaging in a graphene-based waveguide *Japan. J. Appl. Phys.* **58** 050914
[23] An L, Liu H, Sun Q, Huang N and Wang Z 2014 Wavelength conversion in highly nonlinear silicon-organic hybrid slot waveguides *Appl. Opt.* **53** 4886
[24] Ranzani L and José A 2015 Graph-based analysis of nonreciprocity in coupled-mode systems *New J. Phys.* **17** 023024
[25] Koen A, George J P, Jochem V, Kristiaan N, Bart K and Dries V T 2018 Nanophotonic pockels modulators on a silicon nitride platform *Nat. Commun.* **9** 3444
[26] Xie P, Xue M, Wen Y, Li X, Wang X and Liu J 2019 Unveiling electrically tunable characteristics of second-order dispersion in graphene-silicon nitride waveguides *Mod. Phys. Lett.* B **33** 1950053